Journal of Bacteriology

Identification and Characterization of Hemolysin-Like Proteins Similar to RTX Toxin in *Pasteurella pneumotropica*

Hiraku Sasaki, Eiichi Kawamoto, Yoshikazu Tanaka, Takuo Sawada, Satoshi Kunita and Ken-ichi Yagami

J. Bacteriol. **2009, 191(11):3698. DOI: 10.1128/JB.01527-08. Published Ahead of Print 10 April 2009.**

JOURNAL OF BACTERIOLOGY, June 2009, p. 3698–3705 Vol. 191, No. 11
0021-9193/09/$08.00+0 doi:10.1128/JB.01527-08

Identification and Characterization of Hemolysin-Like Proteins Similar to RTX Toxin in *Pasteurella pneumotropica*▽†

Hiraku Sasaki,[1]* Eiichi Kawamoto,[1] Yoshikazu Tanaka,[2] Takuo Sawada,[3] Satoshi Kunita,[4] and Ken-ichi Yagami[4]

Animal Research Center, Tokyo Medical University, Shinjuku, Tokyo, Japan[1]; Department of Veterinary Hygiene[2] and Department of Veterinary Microbiology,[3] Nippon Veterinary and Life Science University, Tokyo, Japan; and Graduate School of Comprehensive Human Science and Laboratory Animal Resource Center, University of Tsukuba, Tsukuba, Ibaraki, Japan[4]

Received 29 October 2008/Accepted 29 March 2009

Pasteurella pneumotropica **is an opportunistic pathogen that causes lethal pneumonia in immunodeficient rodents. The virulence factors of this bacterium remain unknown. In this study, we identified the genes encoding two RTX toxins, designated as *pnxI* and *pnxII*, from the genomic DNA of *P. pneumotropica* ATCC 35149 and characterized with respect to hemolysis. The *pnxI* operon was organized according to the manner in which the genes encoded the structural RTX toxin (*pnxIA*), the type I secretion systems (*pnxIB* and *pnxID*), and the unknown *orf*. The *pnxII* gene was involved only with the *pnxIIA* that coded for a structural RTX toxin. Both the structural RTX toxins of deduced PnxIA and PnxIIA were involved in seven of the RTX repeat and repeat-like sequences. By quantitative PCR analysis of the structural RTX toxin-encoding genes in *P. pneumotropica* ATCC 35149, the gene expression of *pnxIA* was found to have increased from the early log phase, while that of *pnxIIA* increased from the late log to the early stationary phase. As expressed in *Escherichia coli*, both the recombinant proteins of PnxIA and PnxIIA showed weak hemolytic activity in both sheep and murine erythrocytes. On the basis of the results of the Southern blotting analysis, the *pnxIA* gene was detected in 82% of the isolates, while the *pnxIIA* gene was detected in 39%. These results indicate that the products of both *pnxIA* and *pnxIIA* were putative associations of virulence factors in the rodent pathogen *P. pneumotropica*.**

Pasteurella pneumotropica is a gram-negative, rod-shaped bacterium that is frequently isolated from the upper respiratory tracts, digestive tracts, and vaginas of rodents (2, 26). This bacterium is the major cause of pasteurellosis in immunodeficient and immunosuppressed animals, while certain effects on health are not observed in immunocompetent animals (2, 26). For the microbiological control of laboratory rodents, *P. pneumotropica* is one of the pathogens that must be prevented in rodent colonies. In *P. pneumotropica* infections, clinical diseases have generally presented with skin lesions, ophthalmitis, conjunctivitis, and otitis media (2); furthermore, clinical diseases have also been known to lead to fatal pneumonia in immunodeficient animals (15, 24, 26).

Although details of the virulence factors of *P. pneumotropica* are still unavailable, predicted virulence associations have been reported (4, 15, 16, 26). Of these, hemolysis is one of the phenotypic characteristics widely distributed in pathogenic bacteria. In particular, many pathogens that belong to the family *Pasteurellaceae* possess one of the pore-forming protein toxins occurring concurrently with hemolysis—a toxin determined to be a repeat in the structural toxin (RTX toxin) (42). RTX toxins are recognized as members of the type I exoprotein secretion system and were first characterized as hemolysins and leukotoxins produced by *Actinobacillus pleuropneumoniae*, *Aggregatibacter* (*Actinobacillus*) *actinomycetemcomitans*, *Bordetella pertussis*, enterohemorrhagic *Escherichia coli*, and *Mannheimia haemolytica* (11, 12, 42). A structural RTX toxin comprises many copies of glycine-rich nonapeptides on the C-terminal half; these repeats can bind to Ca^{2+}, together with erythrocytes, and several RTX toxins can each act as a hemolysin (7, 32). Further, RTX toxins exhibit cytotoxic activity in a broad range of host cells, including erythrocytes, leukocytes, and epithelial cells (19, 42). Several RTX toxins can reportedly recognize and bind to the β_2 integrin family (21, 27), and the RTX toxin produced by *Vibrio cholerae* has been reported to covalently cross-link with cellular actin (13). Furthermore, several studies have shown that a high concentration of RTX toxins induces necrosis, whereas a low concentration of RTX toxins induces apoptosis (10, 17, 21, 37). Therefore, RTX toxins are considered to be one of the important virulence factors in *Pasteurellaceae*; however, there has been no report on the relevance of RTX toxins in *P. pneumotropica*. In the present study, we report the identification of gene coding in high-molecular-weight proteins that are similar to the RTX toxin family from the genomic DNA of *P. pneumotropica*; they are characterized according to the in vitro expression of genes, as well as observations vis-à-vis hemolytic activity. We also report on the genetic distribution of those RTX toxins in wild-type *P. pneumotropica* strains.

MATERIALS AND METHODS

Bacterial strains and culture media. The *P. pneumotropica* reference strains employed in this study were ATCC 35149, ATCC 12555, CCUG 26450, CCUG 26451, CCUG 26453, and CCUG 36632. The reference strains of the related genera used for comparative analysis were *Actinobacillus muris* CCUG 16938^T, *A. pleuropneumoniae* CCUG 41656^T, *E. coli* RIMD 0509939, *Haemophilus influ-*

* Corresponding author. Mailing address: Animal Research Center, Tokyo Medical University, 6-1-1, Shinjuku, Tokyo, Japan. Phone: 81-3-3351-6141. Fax: 81-3-3350-8659. E-mail: h-sasaki@tokyo-med.ac.jp.

† Supplemental material for this article may be found at http://jb.asm.org/.

▽ Published ahead of print on 10 April 2009.

TABLE 1. Oligonucleotide primers used in this study

Primer	Oligonucleotide sequence (5′–3′)	Target	Position[a]
RI1	CTTTCGGGTGGCGATC	*pnxI*	850–835
RI2	CACCATGGGCACTGAATATTTAG	*pnxI*	1479–1497
RI3	CGCCCAATTATCAGGGAATA	*pnxI*	2561–2580
RI4	TCATTACCCTTTCCCCCAAA	*pnxI*	2722–2703
RI5	TGCCAGCTTCATCGTAGA TT	*pnxI*	3270–3251
RI6	GATAATTAGGGTTGTGGAGATTCTC	*pnxI*	3597–3573
RI7	TACGGGATCCCTAGCTTA ATATAGATTGAT	*pnxI*	3614–3595
RI8	TACGGGATCCATGGAAAAAGAAAAAAAATACCC	*pnxI*	3629–3651
RI9	CTTTCCGTTTTTTCGT TTG	*pnxI*	4267–4248
RI10	CACCTGTTCGTGAAG	*pnxI*	6501–6515
RI11	CAAGGGCAAGAAGTGACAGT	*pnxI*	7541–7560
RII1	TCGGTTCGCATAAT TCC	*pnxII*	489–473
RII2	GCGGAAAATGCGGTAATCTTGG	*pnxII*	1389–1368
RII3	CACCATGGCTACTTTTCTCCAT	*pnxII*	1601–1618
RII4	CTTCACTAGCCTGAAGTGCACC	*pnxII*	1919–1898
RII5	CTTCGCTGCAGAGGGAAAAG	*pnxII*	4758–4778
RII6	GGAGGAAAACCAGGTGGTTTG	*pnxII*	4878–4858
RII7	TCATCGCCAGCTTCCCCAAC	*pnxII*	5418–5399
RII8	GAGCGGTCA TTGAACAAAGCCA	*pnxII*	5679–5718
RII9	GCTTTGTTCAATGACCGC	*pnxII*	5716–5699
RII10	ATTGGCTCCTCCTGCTGGAC	*pnxII*	6141–6160
PPrpo-f	TCGCAAAGTCATTGACGGTCAAG	*rpoB*	216–238
PPrpo-r	ACGAGCCGTAACAAAAGCATCAG	*rpoB*	354–332
EChlyBD-f	GACGGATCCGATGAGTAAATGTAGTTCTC	*hlyB*	19661–19679
EChlyBD-r	AGTGGTACCACGTTCACGTAAAC	*hlyD*	23218–23205
apxIA-f	CATTCGAACTTGGGAACG	*apxIA*	2846–2863
apxIA-r	CCGCCTGAGCCTACAGAT	*apxIA*	3743–3726
apxIIA-f	ATCGCAAATTTAGGTGCT	*apxIIA*	2617–2634
apxIIA-r	ACCAATTCCCAATACGAA	*apxIIA*	3316–3299

[a] The primer positions of *pnxI* and *pnxII* are represented in the nucleotide coordinates of Fig. 1a. The primer positions of *rpoB* (AB461843), *hlyBD* (AB011549), *apxIA* (X68595), and *apxIIA* (M30602) are represented in the nucleotide coordinates of the corresponding gene sequence.

enzae-murium CCUG 6515, and Bisgaard Taxon 17 CCUG 17206. Strains ATCC 35149 and ATCC 12555 were obtained from the American Type Culture Collection (Manassas, VA), and strain RIMD 0509939 was obtained from the Research Institute for Microbial Diseases, Osaka University (Osaka, Japan). The other strains were obtained from the Culture Collection of the University of Göteborg (Göteborg, Sweden).

A total of 44 wild-type strains of *P. pneumotropica* from the upper respiratory tracts of rodents—24 isolates from mice, 18 isolates from rats, 1 isolate from a wild mouse, and 1 from a hamster—were also employed for the examinations. For genetic manipulation, *E. coli* strains DH5α, TOP10, and BL21-AI were employed in this study. All *P. pneumotropica* strains were maintained in a brain heart infusion (BHI) medium (BD, Cockeysville, MD), and transformed *E. coli* bacteria were grown in Luria-Bertani (LB) medium supplemented as necessary with 100 μg/ml ampicillin, 30 μg/ml chloramphenicol, 50 μg/ml kanamycin, 125 μM 5-bromo-4-chloro-3-indolyl-β-D-galactopyranoside (X-Gal), and 1 mM isopropyl-β-D-thiogalactopyranoside (IPTG) for the selection and maintenance of recombinant *E. coli*. For the induction of gene expression in recombinant *E. coli*, 0.1% L-arabinose was added to the LB medium.

Nucleic acid extraction and purification. Plasmid and genomic DNA was extracted according to the method of Sambrook et al. (33). RNA isolation was performed using the cell fraction from the bacterial culture, followed by cell lysis and chloroform-phenol extraction. In brief, bacterial cultures were centrifuged at 15,000 × *g* at 4°C for 5 min; the bacterial pellets were subsequently washed two times and resuspended in 100 μl of RNase-free water. The RNA was isolated using EASYPrep RNA (Takara Bio, Shiga, Japan), according to the manufacturer's instructions.

Construction of clone libraries. The extracted DNA from *P. pneumotropica* ATCC 35149 was partially digested with Sau3AI, and the sizes of the DNA segments were fractionated at 5 to 8 kb on agarose gels. The excised DNA was purified and ligated with a BamHI-digested pUC19 using a T4 DNA ligase (Biodynamics Laboratory, Tokyo, Japan), and the ligation products were transformed into the *E. coli* strain DH5α. The clones were screened using colony hybridization and partial nucleotide sequencing, as described in the subsequent section.

Colony hybridization and Southern blotting. Colony hybridization and Southern blotting were performed, on the basis of the methods of Kuhnert et al. (18). In brief, the digoxigenin-11-dUTP (DIG)-labeled *apxIA* and *apxIIA* probes were generated by the genomic DNA from *A. pleuropneumoniae* CCUG 41656^T, with the primer pair sets apxIA-f and apxIA-r and apxIIA-f and apxIIA-r, respectively (Table 1 lists the oligonucleotide primers used in this study). Colony blotting was performed, followed by lysozyme and proteinase K digestion with alkaline transfer, onto positively charged nylon membranes (GE Healthcare, Amersham, United Kingdom). The prehybridization was performed for 1 h, and subsequently, the hybridization was performed in DIG Easy Hyb hybridization solution (Roche Diagnostics, Mannheim, Germany) containing approximately 0.2 mg/ml of DIG-labeled *apxIA* or *apxIIA* probes at 45°C overnight. Nylon membranes were washed twice for 5 min with 2× saline sodium citrate (SSC; 1× SSC is 0.15 M NaCl plus 0.015 M sodium citrate) buffer containing 0.1% sodium dodecyl sulfate (SDS) under low-stringent conditions; thereafter, they were washed two times for 15 min with 0.5× SSC buffer containing 0.1% SDS under high-stringent conditions. The hybridized clone DNA segments were detected with CDP-Star (Roche Diagnostics), according to the manufacturer's instructions, using a densitograph (model cool saver AE-6955; Atto, Tokyo, Japan).

For the Southern blotting analysis of *P. pneumotropica* RTX genes, the DIG-labeled *pnxIA* and *pnxIIA* probes were generated with primer pairs RI3-RI5 and RII5-RII7 from the genomic DNA of *P. pneumotropica* ATCC 35149, respectively. The genomic DNA from the reference and wild-type strains of *P. pneumotropica* and related genera were digested with HindIII and loaded on agarose gels. Southern blotting was also performed by alkaline transfer onto positively charged nylon membranes (GE Healthcare). The hybridization protocols were based on the method of colony hybridization, with the following modifications. The DIG-labeled *pnxIA* and *pnxIIA* probes were hybridized differently, with HindIII-digested genomic DNA at 40°C and 44°C, respectively. The existence of *pnxIA* and *pnxIIA* genes in the *P. pneumotropica* strains and the related species were also detected with CDP-Star (Roche Diagnostics) using a densitograph (Atto).

DNA sequencing. The nucleotide sequences of the *pnxI* operon and *pnxIIA* were determined with an ABI 310 or ABI 3730XL genetic analyzer (Applied Biosystems, Foster City, CA).

Growth kinetics. *P. pneumotropica* ATCC 35149 was precultured in BHI broth for 18 h, and the growth cells were inoculated into fresh BHI broth at a dilution of 1:100 and incubated at 37°C for up to 13 h, until the cells had progressed to the stationary phase of growth. Samples were collected at 1-h intervals; thereafter, 5- to 10-fold diluted cultures were measured for optical density (OD) at 600 nm (model UV-1600 spectrophotometer; Shimadzu, Kyoto, Japan). Further, the collected samples were employed for the expression analysis of the mRNA of the *pnxIA* and *pnxIIA* genes and the hemolytic analysis of both sheep and murine erythrocytes, as described in the subsequent section.

Reverse transcription PCR and SYBR green-based quantitative PCR assay. Single-stranded cDNA synthesis was performed with a high-capacity cDNA synthesis kit (Applied Biosystems) by using 0.50 μg of DNase I-treated total RNA. The reaction was performed at 25°C for 10 min, followed by 37°C for 120 min and 95°C for 5 min. The synthesized cDNA was employed as a template for real-time quantitative PCR (qPCR). The quantification of *pnxIA* and *pnxIIA* expression was measured with the primer pairs RI3-RI4 and RI5-RI6, respectively. We selected *rpoB* as the reference gene for the qPCR assays of *P. pneumotropica* (38), and the expression of *rpoB* mRNA in *P. pneumotropica* was analyzed with the primer pair PPrpo-f and PPrpo-r. The quantification of gene expression was performed on an Applied Biosystems 7500 real-time PCR system (Applied Biosystems). The qPCR was conducted on 9 μl of 10-fold-diluted reverse-transcribed cDNA and 10 μl of 2× Power SYBR green PCR master mix (Applied Biosystems) with 0.5 μl of 250 nM primers. The thermal cycling conditions were as follows: 2 min at 50°C and subsequently 10 min at 95°C, followed by 40 cycles, with 1 cycle consisting of 15 s at 95°C and 1 min at 60°C. The qPCR was performed in triplicate, and the expressions of *pnxIA* and *pnxIIA* were normalized with the concurrent expression level of *rpoB*. The relative quantification of gene expression was determined by the $2^{-\Delta\Delta}C^{T}$ method (23).

Construction of the PnxIA and PnxIIA expression vectors. All *pnxIA* and *pnxIIA* genes were amplified using the primer pairs RI2-RI6 and RII3-RII9, respectively. The PCR amplicons were purified from agarose gels and cloned into a pENTR/SD/D-TOPO vector (Invitrogen, Carlsbad, CA), according to the manufacturer's instructions. The entry vectors containing *pnxIA* or *pnxIIA* were transformed into TOP10 *E. coli* cells. The entry vectors were purified and recombined with destination vector pDEST17 (Invitrogen), creating fusion proteins bearing an N-terminal six-histidine tag; subsequently, the destination vectors were transformed into TOP10 *E. coli* cells. The resultant expression vectors harboring the *pnxIA* and *pnxIIA* genes were designated as pPNX-IA and pPNX-IIA, respectively. In addition, the coexpression vector of both *pnxIA* and *orf* was also constructed. The genes of *pnxIA* and *orf* were amplified with primer pairs RI2-RI7 and RI8-RI9, respectively, which contained restriction enzyme BamHI recognition sites. The PCR products were digested with BamHI and ligated with each other. Approximately 2.8 kb of the ligation product was separated from an agarose gel and reamplified with the primer pair RI2-RI9. The PCR product was purified from agarose gels and introduced into the entry vector pENTR/SD/D-TOPO. The entry vector was recombined with destination vector pDEST17. The in-frame coexpression vector harboring the *pnxIA* and *orf* genes was designated pPNX-IA′. The construction of all the expression vectors was confirmed by a partial DNA sequence.

Expression and purification of recombinant fusion protein of PnxIA and PnxIIA. The expression vectors were transformed into *E. coli* BL21-AI for the expression of fusion proteins. The recombinant fusion proteins were induced by the addition of 0.1% L-arabinose at the early mid-log phase, and the overnight culture at room temperature was employed to extract the fusion protein, using the following method. *E. coli* cells were harvested by centrifugation (15,000 × *g*, 20 min), and the insoluble fraction of the proteins was dissolved in a denaturant buffer containing 6 M guanidine hydrochloride, 20 mM sodium phosphate (pH 7.8), and 500 mM NaCl. The fusion proteins in denaturant buffer were purified using a Ni-nitrilotriacetic acid purification system (Invitrogen), according to the manufacturer's instructions. The purified denaturing fusion proteins were further rinsed four times with a native wash buffer containing 50 mM NaH_2PO_4 (pH 8.0), 500 mM NaCl, and 20 mM imidazole. The resultant soluble fractions and total proteins were employed for SDS-polyacrylamide gel electrophoresis analysis and a proteolysis assay.

Proteolysis assay. The proteolytic activity of the recombinant proteins was determined by monitoring the caseinolytic activity, according to the method of Cabral et al. (5), with minor modifications. In brief, 40 μl of 2% azocasein containing 50 mM Tris-HCl (pH 8.5) and 20 μl of 4 μg/ml and 40 μg/ml of each recombinant protein were mixed and incubated at 37°C for 3 h. Thereafter, 75 μl of 10% trichloroacetic acid was added to the mixture and incubated at 4°C for 10 min. The mixture was centrifuged at 10,000 × *g* for 10 min, and 100 μl of the supernatant was mixed with an equal volume of 1 N NaOH. The release of azo dye via the hydrolysis of azocasein in the supernatant was measured with the spectrometer UV-1600 at 440 nm. The lysate from the *E. coli* cells that did not have the expression vector was prepared by using a Ni-nitrilotriacetic acid purification system (Invitrogen) and dissolved in 50 mM Tris-HCl (pH 8.5). This lysate was used to correct the absorbance readings of the samples as a control.

Preparation of the recombinant *E. coli* strains for the hemolysis assay. For the hemolysis assay with *E. coli* derivatives, we generated a BL21-AI deletion mutant of the cryptic hemolytic gene *hlyE* (equivalent to *clyA* and *sheA*) (1, 31, 40) with the Quick and Easy *E. coli* gene deletion kit (Gene Bridges, Heidelberg, Germany) according to the manufacturer's instructions. In brief, BL21-AI carrying the λ red expression plasmid pRedET (amp) was grown in LB broth supplemented with 50 μg/ml ampicillin at 30°C for 3 h. Thereafter, 0.1% L-arabinose was inoculated into the culture, and further incubated at 30°C for 2 h. The PCR products containing a kanamycin cassette flanked by FLP recognition sites and the nucleotides of 50-bp homology to the target site in the *hlyE* gene were electroporated into strain BL21-AI. The nucleotide sequences of the 50-bp homology regions in the *hlyE* gene used for Red/ET recombination were as follows: oligo 1, 5′-GAGTATTCACAGGCAGCCTCCGTTTTAGTCGGCGATATTAAAACCTTACT-3′; oligo 2, 5′-CTTTATTCGCTTGTTTAACCGTGTTAGACAGGGTGGTAAAGAAATTCTGC-3′. PCR was used to confirm that the resultant BL21-AI Δ*hlyE*::kan strain was obtained, and the strain was designated as TMU0812. TMU0812 was transformed with pPNX-IA, pPNX-IIA, and pPNX-IA′, and the resultant transformants were used for the hemolysis assay of the crude lysates.

For the hemolysis assay of the intact cells, a coexpression vector of the *hlyB* and *hlyD* genes was constructed. In brief, the *hlyB* and *hlyD* genes were amplified with the primer pair EChlyBD-f- and EChlyBD-r from a total DNA sample of *E. coli* RIMD 0509939. The amplicon of *hlyB* and *hlyD* was digested with BamHI and KpnI. The purified PCR products were ligated with the corresponding sites of pACYCDuet-1 (Merck KGaA, Darmstadt, Germany) using a T4 DNA ligase (Biodynamics Laboratory). TMU0812 cells were transformed with pACYCDuet-1 harboring *hlyB* and *hlyD*, and this strain was designated the TISS strain. The TISS strain was transformed with pPNX-IA, pPNX-IIA, and pPNX-IA′, and the transformants were designated TISS-IA, TISS-IIA, and TISS-IA′, respectively. These strains were then used for the hemolysis assay of the intact cells.

Hemolysis assay. Hemolytic activity was measured by the detection of hemoglobin released from sheep and murine erythrocytes, according to the method of Flieger et al. (9). Defibrinated sheep and murine blood was obtained from Nippon Bio-Test Laboratories, Inc. (Tokyo, Japan) and Kohjin Bio (Saitama, Japan), respectively. All the erythrocytes used for the following examinations were washed in triplicate with sterilized 150 mM NaCl that had been supplemented with 50 mM $CaCl_2$. To observe the hemolytic activity of *P. pneumotropica* or the TISS derivatives of the *E. coli* strain on plates, we routinely employed sheep blood agar (SBA), by which 50 ml of washed sheep erythrocytes was added to 1 liter of BHI agar or LB agar with 100 μg/ml of ampicillin and 30 μg/ml of chloramphenicol, respectively. For the visualization of hemolytic activity on the plates, we employed commercially available SBA purchased from Nissui (Tokyo, Japan) and Eiken (Tokyo, Japan). *E. coli* and *P. pneumotropica* ATCC 35149 cells were inoculated onto SBA plates and incubated at 37°C for 48 h and 72 h, respectively.

For the hemolytic analysis of *P. pneumotropica* ATCC 35149, bacterial cells were harvested through centrifugation (15,000 × *g*, 10 min) and washed twice with 150 mM NaCl. The washed sheep and murine erythrocytes were diluted with 150 mM NaCl at 1.25% and 2.5%, respectively. A total of 200 μl of the bacterial solution was mixed with 800 μl of the diluted erythrocytes. The mixture was incubated for 2 h at 37°C; thereafter, the mixture was centrifuged (800 × *g*, 2 min), and the supernatant was measured with the spectrometer UV-1600 at 415 nm. The quantification results of the hemolytic activity in *P. pneumotropica* ATCC 35149 were estimated at optical densities at 415 nm and 600 nm (OD_{415} and OD_{600}, respectively).

To analyze the hemolytic activity of the recombinant *E. coli*, we used the TMU0812 strain and TISS derivatives for the crude lysates and intact cells, respectively. In brief, bacterial cells were cultured in LB broth for 3 h; 0.1% of L-arabinose was added to the culture, and the *E. coli* cells were further incubated for 2 h. For the analysis of the crude lysates, TMU0812 derivatives were suspended in buffer containing 50 mM Tris-HCl (pH 8.0) and 150 mM NaCl and sonicated on ice. The protein concentration of the crude lysate was measured with the protein assay rapid kit Wako (Wako Pure Chemical, Osaka, Japan). Crude lysate solution (200 μl) was mixed with 800 μl of the diluted erythrocytes. The mixture was incubated for 2 h at 37°C and subsequently centrifuged at 800 × *g* for 2 min. The hemoglobin release in the supernatant was measured at 415 nm.

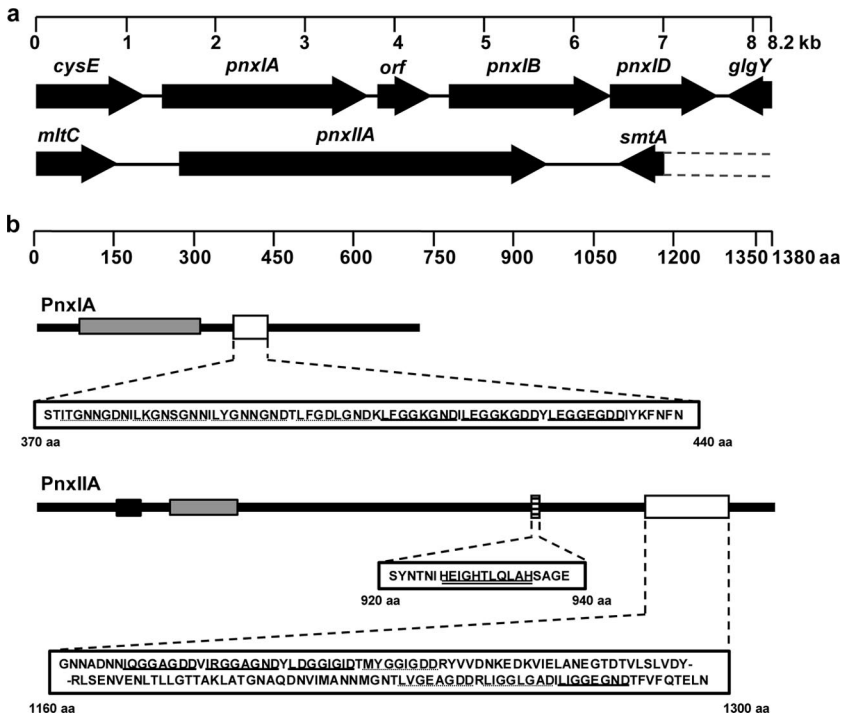

FIG. 1. Predicted genetic map of *Pasteurella pneumotropica* ATCC 35149 *pnxI* operon and *pnxIIA* (a) and structure of PnxIA and PnxIIA (b). In approximately the 6-kb region of the *pnxI* operon, there are four putative open reading frames. Putative hemolysin-type Ca^{2+}-binding regions are indicated by white boxes. In the lower section, the RTX repeats of the glycine-rich regions and the repeat-like regions that are similar but not completely identical to the RTX repeats are indicated by solid and dotted lines, respectively. A white box filled with hatched lines contains the Zn^{2+}-binding domain, and the serralysin-like sequence is indicated by double lines in the lower section. A gray and black box indicates predicted hydrophobic and hydrophilic regions.

To assess the hemolytic activity of the intact cells, TISS, TISS-IA, and TISS-IIA cells were incubated and induced in the same manner as described above. Thereafter, the OD_{600} of the culture was adjusted to 1.0, and the *E. coli* cells were resuspended in 150 mM NaCl solution. A total of 200 μl of the cell solution was mixed with 800 μl of the washed erythrocytes. The mixture was incubated at 37°C for 2 h and subsequently centrifuged at 800 × *g* for 2 min. The hemoglobin release in the supernatant was measured at 415 nm.

Nucleotide sequence accession numbers. The nucleotide sequences of *pnxIA*, *pnxIB*, *pnxID*, *orf*, and *pnxIIA* were deposited in GenBank through DDBJ, and the accession numbers assigned were AB466276, AB466277, AB466278, AB466279, and AB466280, respectively.

RESULTS

Identification of the genes encoding RTX toxins. In the preliminary experiment, weak hybridized signals were obtained from the genomic DNA of *P. pneumotropica* ATCC 35149 through dot blotting with the *apxIA* and *apxIIA* probes, according to the methods of Kuhnert et al. (18). Subsequently, the clone library was constructed and screened with these probes. There were several clones that showed weak signals, including unspecific signals by the colony hybridization with the *apxIIA* probe. However, most of the clones were not contained, similarly to the genes encoding the RTX sequence; therefore, we finally screened the clones based on partial nucleotide sequencing. There were two clones containing 6.3-kb and 5.4-kb insertions that were included similarly to the consensus sequences of the RTX toxin. We completely sequenced these two clones by primer walking and further sequenced the uninserted regions from the genomic DNA of *P. pneumotropica* ATCC 35149 by inverse PCR. Two genes encoding proteins similar to the RTX toxins were finally identified and designated *pnxI* and *pnxII* (Fig. 1a). The *pnxI* operon contained four open reading frames designated *pnxIA*, *orf*, *pnxIB*, and *pnxID*. The structural toxin was encoded by *pnxIA* genes that contained a TAG stop codon, and an 80-kDa sequence of deduced amino acids from *pnxIA* was partially found to have 50% similarity with the putative Ca^{2+}-binding hemolysin protein identified in *Pseudomonas aeruginosa* (accession no. ACD38651), via a protein BLAST search. The deduced amino acid sequences of the *pnxIB* and *pnxID* genes were predicted to code for the type I secretion systems of the ATP-binding cassette (ABC) protein and membrane fusion protein (MFP), respectively. The ABC protein encoded by the *pnxIB* gene exhibited 87% similarity with the LktB protein in *Mannheimia haemolytica* (AAL12791) and *Mannheimia glucosida* (AAL12803), and the MFP encoded by *pnxID* exhibited 68% similarity with the HlyD protein in uropathogenic *E. coli* (YP_672390). However, an unknown protein encoded by *orf* showed a low score (35.0) and had 45% similarity with the hypothetical protein in *Geobacillus thermodenitrificans* (YP_001124547). The consensus sequence of RTX toxin (L/I/F-X-G-G-X-G-N/D-X, where X represents any of the amino acids) was found in PnxIA three times, and the RTX-like sequence (L/I-X-G-*N*-X-G-N/D-X [the alternate amino acid residue is italicized]) that was not completely identical to the consensus sequence but highly similar to these sequences was also found in PnxIA four times (Fig. 1b). These regions—both the RTX and the RTX-like sequence—were

also the regions that were putative hemolysin-type Ca^{2+}-binding regions. A 5.4-kb segment of the *pnxII* gene was predicted to involve only *pnxIIA* that codes for a structural RTX toxin (Fig. 1a). A 151-kDa segment of deduced amino acid sequences from the *pnxIIA* gene partially exhibited 50% similarity with the Ca^{2+}-binding domain protein identified in *Haemophilus parasuis* (ZP_02478400) via a protein BLAST search. The RTX consensus sequence was found in PnxIIA four times; the RTX-like sequence (*L*/*M*-X-G-*G*/*E*-X-G-*D*/*A*-X [the alternate amino acid residues are italicized]) was also found three times (Fig. 1b). In the predicted amino acid sequence of PnxIIA, the unique sequence (H-E-I-G-H-T-L-Q-L-A-H) that was similar to the serralysin motif (H-E-X-X-H-X-X-G-X-X-H) (25) was found in the C-terminal half of PnxIIA (Fig. 1b). The region that contained a serralysin-like sequence indicated the Zn^{2+}-binding domain. In the N-terminal half of both PnxIA and PnxIIA, the hydrophobic regions that are required for pore formation were observed (Fig. 1b). In the case of PnxIIA, approximately 40 amino acid residues existed in the hydrophilic regions that were similar to the outer membrane transporter identified in *Enterobacter* sp. (YP_001165485), and these regions might be related to extracellular secretion.

The gene code for an activation of the protoxin, which is generally denoted with the letter *C*, was not found in the *pnxI* operon, *pnxIIA*, or neighboring genes (Fig. 1a). This gene functions to acylate the structural toxin; further, the putative acylation sites that were conserved in the structural RTX toxins (14, 36) were not found in either PnxIA or PnxIIA. These results indicate that the genes encoding RTX toxins in *P. pneumotropica* have a structure unique to the RTX toxin family.

Expression analysis of *pnxIA* and *pnxIIA* in *P. pneumotropica* ATCC 35149. For the analysis of the expression of genes encoding RTX toxins, we employed the SYBR green-based qPCR method with primer pairs targeting the gene encoding the Ca^{2+}-binding regions in structural toxins. Both the genes in *P. pneumotropica* ATCC 35149 were confirmed to be actually expressed when cultured in BHI medium. The relative quantification of the gene expression of *pnxIA* increased from the early log phase, while that of *pnxIIA* increased from the late log phase to the early stationary phase (Fig. 2b). Simultaneously, the hemolytic activity of the bacterial cells in washed sheep or murine erythrocytes monitored the released hemoglobin and was estimated at OD_{415}/OD_{600}. The rate of hemoglobin release was found to increase gradually, from approximately the early log phase; following the late log phase, hemoglobin was continuously released from both the sheep and murine erythrocytes at a high rate (Fig. 2c). However, an additional 2 h of incubation delayed hemoglobin release (Fig. 2c) compared with the growth rate and the gene expression. These results indicate that *P. pneumotropica* ATCC 35149 possesses the capability to lyse erythrocytes; they also indicate that the erythrocyte lysis patterns of the bacterial cells are similar to the expression patterns of the RTX toxins.

Expression and characterization of recombinant PnxIA and PnxIIA. To determine the characteristics of PnxIA and PnxIIA, we constructed the expression vectors pPNX-IA and pPNX-IIA, respectively, and transformed them into *E. coli* strain BL21-AI. Both the purified recombinant RTX toxins were unstable in the solution, and the minor bands that indicated the putative degradation of both the recombinant RTX toxins

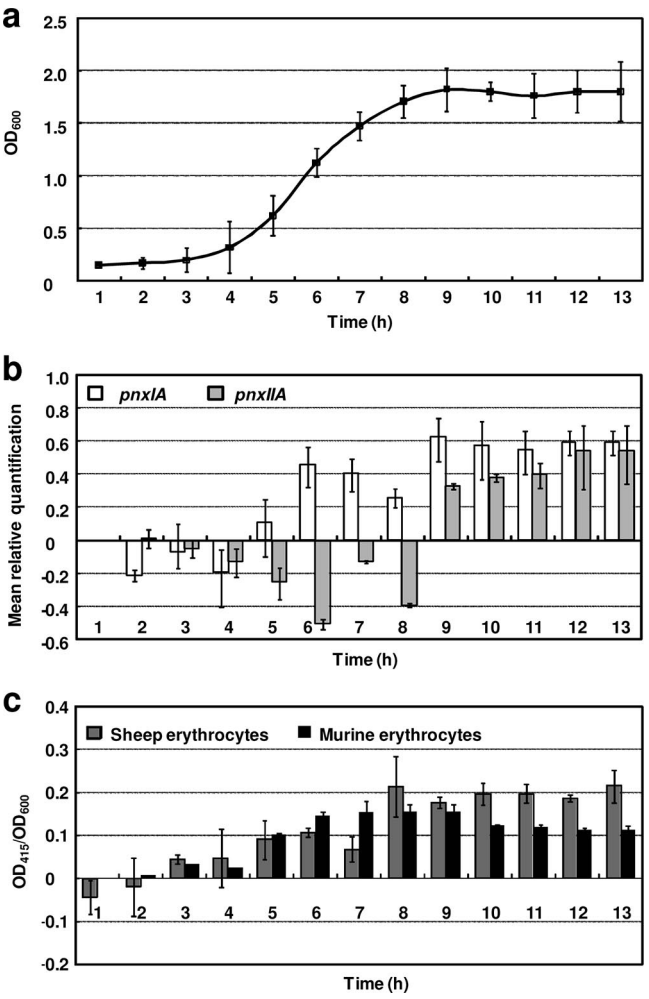

FIG. 2. Changes in growth rate (a), mean relative quantification of the expression of the *pnxIA* and *pnxIIA* genes (b), and the rate of hemoglobin release from the sheep and murine erythrocytes (c) in the case of *Pasteurella pneumotropica* ATCC 35149 cultured in BHI broth at 37°C. The growth rate was measured at OD_{600}. Gene expression was determined by SYBR green I-based quantitative PCR. Hemoglobin release was monitored at OD_{415}, followed by an additional incubation in the sheep or murine erythrocytes at 37°C for 2 h; the rate of hemoglobin release was determined by dividing the OD_{415} values by the OD_{600} values.

and the contaminations were observed on the gels (Fig. 3). In particular, the yield of recombinant PnxIA was lower than that of recombinant PnxIIA. The native recombinant PnxIA and PnxIIA proteins were used to examine the proteolytic activity toward azocasein; however, neither recombinant protein, at concentrations of 4 to 40 μg/ml, showed proteolytic activity vis-à-vis the substrate (data not shown).

To characterize PnxIA and PnxIIA, we employed the crude cell lysate from the TMU0812 strain (BL21-AI Δ*hlyE*::kan), harboring pPNX-IA and pPNX-IIA directly in the functional analysis. In general, many types of RTX protoxin are activated by the acylation gene product, and the activated RTX toxin functions as a cytotoxic protein (14, 36, 42). However, the gene-coding acylation protein was not found in the *pnxI* operon, *pnxIIA*, or the neighboring genes; therefore, the crude

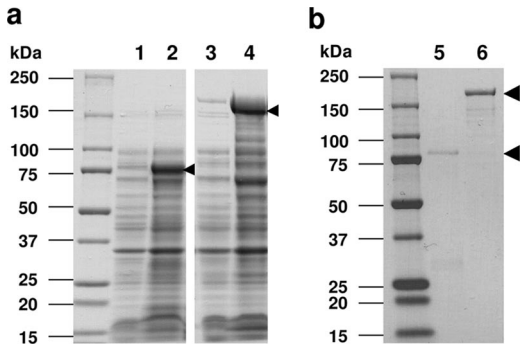

FIG. 3. Induced expression analysis of the *Pasteurella pneumotropica pnxIA* and *pnxIIA* genes in *E. coli* (a) and purified recombinant fusion proteins of PnxIA and PnxIIA (b). Coomassie blue-stained SDS-polyacrylamide gel electrophoresis (5 to 20%) analysis of the following proteins. Lane 1, total protein from *E. coli* transformed with pPNX-IA before induction; lane 2, total protein from *E. coli* transformed with pPNX-IA induced by 0.1% L-arabinose; lane 3, total protein from *E. coli* transformed with pPNX-IIA before induction; lane 4, total protein from *E. coli* transformed with pPNX-IIA induced by 0.1% L-arabinose; lane 5, purified fusion protein of PnxIA; lane 6, purified fusion protein of PnxIIA. Arrowheads indicate the positions of the recombinant fusion proteins.

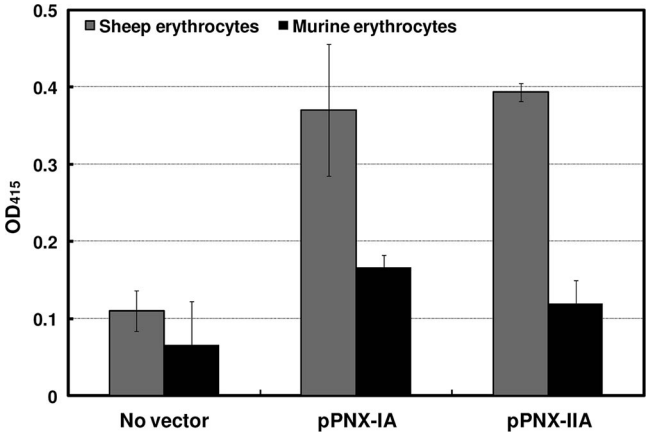

FIG. 4. Hemoglobin release from the sheep and murine erythrocytes cultured with the crude lysates prepared from the TMU0812 strain, TMU0812 harboring pPNX-IA, and pPNX-IIA supplemented with 50 mM $CaCl_2$.

lysates from recombinant *E. coli* cells in which the *pnxIA* or *pnxIIA* genes were expressed were employed to observe hemolytic activities. Figure 4 shows the rate of hemoglobin release when the crude lysates from the TMU0812 strain expressing the *pnxIA* or *pnxIIA* genes were cultured in washed sheep or murine erythrocytes. The crude lysates from TMU0812 cells expressing either of the two genes were found to exhibit a higher rate of hemoglobin release than the lysates from the TMU0812 cells lacking the expression vector. Furthermore, the unknown-function gene designated as *orf* was found in the *pnxI* operon, and the coexpression vector pPNX-IA′ containing both the *pnxIA* and *orf* genes was also examined. However, the rate of hemoglobin release by the crude lysate from the TMU0812 cells harboring pPNX-IA′ was not significantly different from that of the crude lysate from the TMU0812 cells harboring *pnxIA* (0.28 ± 0.08). Furthermore, we modified the TMU0812 strain for the hemolysis assay of intact cells. The *E. coli* hemolysin transport proteins HlyB and HlyD were coexpressed together with PnxIA or PnxIIA in TMU0812. Although recombinant fusion proteins were not exactly detected in the supernatant by Western blotting, both TISS-IA and TISS-IIA cells showed weak hemolytic activity in the erythrocytes (see Fig. S1a in the supplemental material). Images of TISS cells harboring the three expression vectors, as well as those of *P. pneumotropica* ATCC 35149 streaked on an SBA plate are provided (see Fig. S1b and S1c in the supplemental material). The TISS cells harboring the structural RTX protein expression vector on the plate showed weak hemolytic activity, while the TISS cells lacking the structural RTX protein expression vector showed insignificant hemolytic activity. These results indicate that both the RTX toxins are related to the hemolysis of the host strain *P. pneumotropica*.

Distribution of *pnxIA* and *pnxIIA* genes in wild-type strains of *P. pneumotropica*. In this study, many wild-type strains of *P. pneumotropica* were confirmed to possess one of two genes encoding the RTX toxins; otherwise, only reference strains ATCC 12555 and CCUG 36632 were found to possess the *pnxIA* and *pnxIIA* genes, respectively (see Fig. S2 in the supplemental material). Neither of the genes was detected in reference strains CCUG 26450, CCUG 26451, or CCUG 26453, and no signals were observed in the genomic DNA of the related strains *A. muris* CCUG 16938^T, *H. influenzae-emurium* CCUG 6515, or Bisgaard Taxon 17 CCUG 17206 by Southern blotting analysis (see Fig. S2 in the supplemental material).

Table 2 summarizes the distribution of the genes encoding two RTX toxins in the *P. pneumotropica* isolates sorted on the basis of their isolation from either mice or rats. Many of the *P. pneumotropica* isolates were confirmed to possess one of the genes encoding RTX toxins. In brief, greater than 80% of the tested isolates were confirmed to possess the *pnxIA* gene, and the *pnxIIA* gene was detected in approximately 40% of the isolates. In all, 36% of the isolates were confirmed to possess both genes encoding RTX toxins. There was no significant difference in the number of detected isolates by the *pnxIA* probe between the isolates from mice and rats. However, the *pnxIIA* gene was detected in 54% of the isolates from mice; otherwise, that gene was detected in only 17% of the isolates from rats. These results indicate that many wild-type strains possess one of each gene; they also suggest that the distribution of these genes was uneven among the host rodents.

TABLE 2. Percentages of the *Pasteurella pneumotropica* isolates harboring the *pnxIA* and *pnxIIA* genes from mice and rats

Animal	% isolates positive for[a]:		
	pnxIA (82[c])	*pnxIIA* (39[c])	*pnxIA* + *pnxIIA*[b] (36[c])
Mouse	75	54	50
Rat	89	17	17

[a] RTX toxins determined by Southern blotting are represented. The percentages of positive isolates are from the total mouse and rat isolates.
[b] Only the *pnxIA* and *pnxIIA* genes were detected.
[c] Percentages of total isolates include isolates from mice, rats, a wild mouse, and a hamster.

DISCUSSION

Many pathogens that belong to *Pasteurellaceae* are reported to produce an RTX toxin; one of their known features is the ability to lyse erythrocytes (11, 12, 42). In this study, we focused on the hemolytic activity of the structural RTX toxins found in *P. pneumotropica* ATCC 35149. In former studies, reference strains of *P. pneumotropica* were found not to show hemolytic activity on blood agar (2, 26). In liquid culture, however, strain ATCC 35149 was found to possess an obvious ability to lyse erythrocytes (Fig. 2c); in addition, ATCC 35149 cells showed weak hemolytic activity on washed SBA and commercially available SBA supplemented with $CaCl_2$ at 37°C for 72 h of incubation (see Fig. S1c in the supplemental material). Furthermore, several studies have revealed hemolysis in wild-type strains of *P. pneumotropica* (16, 34); these results suggest that reference strain ATCC 35149, as well as several strains of *P. pneumotropica*, are weak hemolytic bacteria. Further, both of the two identified RTX toxins were involved with the putative hemolysin-type Ca^{2+}-binding regions, and as each of the RTX toxins expressed in the *E. coli* cells, both the crude lysates showed weak hemolytic activity in the erythrocytes. Therefore, PnxIA and PnxIIA were considered to act as potential hemolysins in *P. pneumotropica*.

Most of the gene clusters in RTX toxin are denoted with a *C* for the activation of protoxin, *A* for structural toxins, and *BD* for type I secretion systems; many of them are reported to form *CABD* within the same site (42). In pathogenic *E. coli* hemolysin-encoding *hlyA*, protoxin could bind but not lyse erythrocytes, unless the protoxin was acylated by the product of the *hlyC* gene (3). In addition, many of the genes encoding RTX-like exoprotein, including nontoxic members of the RTX protein family, were also involved with the exporter protein and the activity regulator protein; these two genes were located at the same site and were together due to a genetic linkage (8, 39). In this study, one of the candidates that activated PnxIA was initially considered to be the protein encoded by the *orf* gene; however, the coexpression of *pnxIA* and *orf* in *E. coli* cells was found not to be significantly different from the expression of the *pnxIA* gene alone in terms of hemolysis. The hypothetical protein encoded by the *orf* gene was partially similar to the peptide transporter in *Clostridium botulinum* (35). Therefore, the protein encoded by the *orf* gene was considered to be related to the ABC transporter. The genetic code for the activation of structural toxins was not found and identified; however, the expression of the recombinant structural toxin alone in *E. coli* cells was found to show weak hemolysis.

One of the hypotheses might be that PnxIA and PnxIIA were activated by the genetically unlinked protein that is intracellularly produced in *P. pneumotropica* and *E. coli* cells. The other hypothesis is that PnxIA and PnxIIA were, in themselves, already in their active forms. A 100-kDa sequence of Ca^{2+}-dependent bacteriocin that was involved in the consensus RTX sequence in *Rhizobium leguminosarum* was encoded by a single gene that was unlinked to any of the activity regulator genes (30). The RTX-like metalloprotease produced by *Erwinia carotovora* also was encoded by the *prt1* gene alone, and the expression of *prt1* itself, in recombinant *E. coli* cells, showed a high level of protease activity (20). In both PnxIA and PnxIIA, putative acylation sites that were found in strongly cytotoxic types of RTX toxins (36) were found not to be involved. Unlike these RTX toxins, the structural RTX toxins found in *P. pneumotropica* might be activated by different mechanisms.

In the C-terminal half of PnxIIA, the existence of a Zn^{2+}-binding domain was observed (Fig. 1b). One of the zinc metalloproteases produced by *Serratia marcescens* and *P. aeruginosa* is considered a member of the serralysin family (25). The structural features of serralysin involve two domains in both termini of the amino acid sequence, namely, the Zn^{2+}-binding domain (H-E-X-X-H-X-X-G-X-X-H) and the Ca^{2+}-binding domain (G-G-X-G-X-D), which existed in the N and C termini, respectively. In particular, the sequence of the Ca^{2+}-binding domain in serralysin is also conserved in the RTX toxin family, and these regions are reportedly concerned with extracellular secretion (22). The secretion of RTX toxins is known to involve the type I exoprotein secretion system, which mediates the membrane components in bacterial cell membranes, including the outer membrane protein (OMP), MFP, and ABC protein (29, 43). OMP generally is encoded by *tolC*, which is reportedly located at a distance from the RTX operon and unlinked to the gene coding for an RTX toxin (41). In the *pnxI* operon, the ABC protein and MFP are encoded by *pnxIB* and *pnxID*, respectively, while these genes are not found within the neighboring genes of *pnxIIA*. The unrelated toxin containing the Ca^{2+}-binding domain was found to be secreted through type I secretion systems in species that were different from the parent strains (6). For example, the secretion of the RTX toxin ApxIIA by *A. pleuropneumoniae* that lacked type I secretion systems in its coding gene region were secreted via ApxIB and ApxID (11). Further, the hydrophilic regions in the N-terminal half of the PnxIIA protein were involved in the regions that were partially homologous to the periplasmic protein TonB. Thus, the PnxIIA protein was predicted to be secreted via genetically unlinked secretion systems in *P. pneumotropica*. Further, the sequences of the Zn^{2+}-binding domain, as found in PnxIIA, were similar to those of the serralysin family but not completely similar in terms of the consensus sequence. In this study, native recombinant PnxIIA did not show any proteolytic activity toward azocasein, suggesting that differences in the sequence were related to proteolytic activity.

In managing infected laboratory rodents, *P. pneumotropica* is one of the pathogens that should be routinely monitored, especially among immunodeficient rodents. However, its taxonomical classification is uncertain, and the exact name of the genus has not been formally given (28). Therefore, the genetic and biochemical characteristics of wild-type strains of *P. pneumotropica* were heterogenous and diversified (34). A method based on the detection and identification of certain virulence factors in isolates should be developed. To monitor this pathogen, the RTX toxins determined in this study were considered to be candidates for the virulence factor.

Many RTX toxins exhibit hemolytic activity; however, cytotoxicity toward a broad range of host cells, including leukocytes and other cells, directly affects the health of the host animals. For both PnxIA and PnxIIA, the mechanisms underlying cytotoxic activity vis-à-vis host cells remain elusive. The detailed functions of RTX toxins found in *P. pneumotropica* should be clarified in future studies.

ACKNOWLEDGMENT

This study was partially supported by a grant-in-aid (20700369) from the Ministry of Education, Culture, Sports, Science, and Technology, Japan.

REFERENCES

1. **Atkins, A., N. R. Wyborn, A. J. Wallace, T. J. Stillman, L. K. Black, A. B. Fielding, M. Hisakado, P. J. Artymiuk, and J. Green.** 2000. Structure-function relationships of a novel bacterial toxin, hemolysin E. J. Biol. Chem. **275:**41150–41155.
2. **Baker, D. D.** 1998. Natural pathogens of laboratory mice, rats, and rabbits and their effects on research. Clin. Microbiol. Rev. **11:**231–266.
3. **Bauer, M., and R. A. Welch.** 1996. Association of RTX toxins with erythrocytes. Infect. Immun. **64:**4665–4672.
4. **Boot, R., H. Thuis, and J. S. Teppema.** 1993. Hemagglutination by *Pasteurellaceae* isolated from rodents. Zentralbl. Bakteriol. **279:**259–273.
5. **Cabral, C. M., A. Cherqui, A. Pereira, and N. Simões.** 2004. Purification and characterization of two distinct metalloproteases secreted by the entomopathogenic bacterium *Photorhabdus* sp. strain Az29. Appl. Environ. Microbiol. **70:**3831–30838.
6. **Duong, F., A. Lazdunski, and M. Murgier.** 1996. Protein secretion by heterologous bacterial ABC-transporters: the C-terminus secretion signal of the secreted protein confers high recognition specificity. Mol. Microbiol. **21:**459–470.
7. **Felmlee, T., S. Pellett, and R. A. Welch.** 1985. Nucleotide sequence of an *Escherichia coli* chromosomal hemolysin. J. Bacteriol. **163:**94–105.
8. **Ffrench-Constant, R. H., N. Waterfield, V. Burland, N. T. Perna, P. J. Daborn, D. Bowen, and F. R. Blattner.** 2000. A genomic sample sequence of the entomopathogenic bacterium *Photorhabdus luminescens* W14: potential implications for virulence. Appl. Environ. Microbiol. **66:**3310–3329.
9. **Flieger, A., K. Rydzewski, S. Banerji, M. Broich, and K. Heuner.** 2004. Cloning and characterization of the gene encoding the major cell-associated phospholipase A of *Legionella pneumophila*, *plaB*, exhibiting hemolytic activity. Infect. Immun. **72:**2648–2658.
10. **Fong, K. P., C. M. Pacheco, L. L. Otis, S. Baranwal, I. R. Kieba, G. Harrison, E. V. Hersh, K. Boesze-Battaglia, and E. T. Lally.** 2006. *Actinobacillus actinomycetemcomitans* leukotoxin requires lipid microdomains for target cell cytotoxicity. Cell. Microbiol. **8:**1753–1767.
11. **Frey, J.** 2008. RTX toxin-determined virulence of *Pasteurellaceae*, p. 133–144. *In* P. Kuhnert and H. Christensen (ed.), *Pasteurellaceae*. Horizon Scientific Press, Norwich, United Kingdom.
12. **Frey, J., and P. Kuhnert.** 2002. RTX toxins in *Pasteurellaceae*. Int. J. Med. Microbiol. **292:**149–158.
13. **Fullner, K. J., and J. J. Mekalanos.** 2000. *In vivo* covalent cross-linking of cellular actin by the *Vibrio cholerae* RTX toxin. EMBO J. **19:**5315–5323.
14. **Hackett, M., L. Guo, J. Shabanowitz, D. F. Hunt, and E. L. Hewlett.** 1994. Internal lysine palmitoylation in adenylate cyclase toxin from *Bordetella pertussis*. Science **266:**433–435.
15. **Hart, M. L., D. A. Mosier, and S. K. Chapes.** 2003. Toll-like receptor 4-positive macrophages protect mice from *Pasteurella pneumotropica*-induced pneumonia. Infect. Immun. **71:**663–670.
16. **Hooper, A., and A. Sebesteny.** 1974. Variation in *Pasteurella pneumotropica*. J. Med. Microbiol. **7:**137–140.
17. **Korostoff, J., J. F. Wang, I. Kieba, M. Miller, B. J. Shenker, and E. T. Lally.** 1998. *Actinobacillus actinomycetemcomitans* leukotoxin induces apoptosis in HL-60 cells. Infect. Immun. **66:**4474–4483.
18. **Kuhnert, P., B. Heyberger-Meyer, A. P. Burnens, J. Nicolet, and J. Frey.** 1997. Detection of RTX toxin genes in gram-negative bacteria with a set of specific probes. Appl. Environ. Microbiol. **63:**2258–2265.
19. **Kuhnert, P., H. Berthoud, R. Straub, and J. Frey.** 2003. Host cell specific activity of RTX toxins from haemolytic *Actinobacillus equuli* and *Actinobacillus suis*. Vet. Microbiol. **92:**161–167.
20. **Kyöstiö, S. R., C. L. Cramer, and G. H. Lacy.** 1991. *Erwinia carotovora* subsp. *carotovora* extracellular protease: characterization and nucleotide sequence of the gene. J. Bacteriol. **173:**6537–6546.
21. **Lally, E. T., R. B. Hill, I. R. Kieba, and J. Korostoff.** 1999. The interaction between RTX toxins and target cells. Trends Microbiol. **7:**356–361.
22. **Létoffé, S., P. Delepelaire, and C. Wandersman.** 1990. Protease secretion by *Erwinia chrysanthemi*: the specific secretion functions are analogous to those of *Escherichia coli* alpha-haemolysin. EMBO J. **9:**1375–1382.
23. **Livak, K. J., and T. D. Schmittgen.** 2001. Analysis of relative gene expression data using real-time quantitative PCR and the $2^{-\Delta\Delta CT}$ method. Methods **25:**402–408.
24. **Macy, J. D., Jr., E. C. Weir, S. R. Compton, M. J. Shlomchik, and D. G. Brownstein.** 2000. Dual infection with *Pneumocystis carinii* and *Pasteurella pneumotropica* in B cell-deficient mice: diagnosis and therapy. Comp. Med. **50:**49–55.
25. **Maeda, H., and K. Morihara.** 1995. Serralysin and related bacterial proteinase. Methods Enzymol. **248:**395–412.
26. **Manning, P. J., R. F. DiGiacomo, and D. DeLong.** 1989. Pasteurellosis in laboratory animals, p. 263–302. *In* C. Adlam and J. M. Rutter (ed.), Pasteurella and pasteurellosis. Academic Press, London, United Kingdom.
27. **Morova, J., R. Osicka, J. Masin, and P. Sebo.** 2008. RTX cytotoxins recognize beta2 integrin receptors through N-linked oligosaccharides. Proc. Natl. Acad. Sci. USA **105:**5355–5360.
28. **Mutters, R., H. Christensen, and M. Bisgaard.** 2005. Genus I. *Pasteurella* Trevisan 1887, p. 857–866. *In* D. J. Brenner, N. R. Krieg, J. T. Staley, and G. M. (ed.) Bergey's manual of systematic bacteriology, 2nd ed., vol. 2, part B. Springer, New York, NY.
29. **Omori, K., and A. Idei.** 2003. Gram-negative bacterial ATP-binding cassette protein exporter family and diverse secretory proteins. J. Biosci. Bioeng. **95:**1–12.
30. **Oresnik, I. J., S. Twelker, and M. F. Hynes.** 1999. Cloning and characterization of a *Rhizobium leguminosarum* gene encoding a bacteriocin with similarities to RTX toxins. Appl. Environ. Microbiol. **165:**2833–2840.
31. **Oscarsson, J., Y. Mizunoe, B. E. Uhlin, and D. J. Haydon.** 1996. Induction of haemolytic activity in *Escherichia coli* by the *slyA* gene product. Mol. Microbiol. **20:**191–199.
32. **Ostolaza, H., and F. Goñi.** 1995. Interaction of the bacterial protein toxin α-haemolysin with model membranes: protein binding does not always lead to lytic activity. FEBS Lett. **371:**303–306.
33. **Sambrook, J., and D. W. Russell.** 2001. Molecular cloning: a laboratory manual, 3rd ed. Cold Spring Harbor Laboratory Press, Cold Spring Harbor, NY.
34. **Sasaki, H., E. Kawamoto, E. Okiyama, H. Ueshiba, K. Mikazuki, H. Amao., and T. Sawada.** 2006. Molecular typing of *Pasteurella pneumotropica* isolated from rodents by amplified 16S ribosomal DNA restriction analysis and pulsed-field gel electrophoresis. Microbiol. Immunol. **50:**265–272.
35. **Smith, T. J., K. K. Hill, B. T. Foley, J. C. Detter, A. C. Munk, D. C. Bruce, N. A. Doggett, L. A. Smith, J. D. Marks, G. Xie, and T. S. Brettin.** 2007. Analysis of the neurotoxin complex genes in *Clostridium botulinum* A1–A4 and B1 strains: BoNT/A3, /Ba4 and /B1 clusters are located within plasmids. PLoS ONE **2:**e1271.
36. **Stanley, P., L. C. Packman, V. Koronakis, and C. Hughes.** 1994. Fatty acylation of two internal lysine residues required for the toxic activity of *Escherichia coli* hemolysin. Science **266:**1992–1996.
37. **Sun, Y. D., K. D. Clinkenbeard, C. Clarke, L. Cudd, S. K. Highlander, and S. M. Dabo.** 1999. *Pasteurella haemolytica* leukotoxins induced apoptosis of bovine lymphocytes involves DNA fragmentation. Vet. Microbiol. **65:**153–166.
38. **Tasara, T., and R. Stephan.** 2007. Evaluation of housekeeping genes in *Listeria monocytogenes* as potential internal control references for normalizing mRNA expression levels in stress adaptation models using real-time PCR. FEMS Microbiol. Lett. **26:**265–272.
39. **Uphoff, T. S., and R. A. Welch.** 1990. Nucleotide sequencing of the *Proteus mirabilis* calcium-independent hemolysin genes (*hpmA* and *hpmB*) reveals sequence similarity with the *Serratia marcescens* hemolysin genes (*shlA* and *shlB*). J. Bacteriol. **172:**1206–1216.
40. **Wallace, A. J., T. J. Stillman, A. Atkins, S. J. Jamieson, P. A. Bullough, J. Green, and P. J. Artymiuk.** 2000. *E. coli* hemolysin E (HlyE, ClyA, SheA): X-ray crystal structure of the toxin and observation of membrane pores by electron microscopy. Cell **100:**265–276.
41. **Wandersman, C., and P. Delepelaire.** 1990. TolC, an *Escherichia coli* outer membrane protein required for hemolysin secretion. Proc. Natl. Acad. Sci. USA **87:**4776–4780.
42. **Welch, R. A.** 2001. RTX toxin structure and function: a story of numerous anomalies and few analogies in toxin biology. Curr. Top. Microbiol. Immunol. **257:**85–111.
43. **Young, J., and I. B. Holland.** 1999. ABC transporter: bacterial exporters revisited five years on. Biochim. Biophys. Acta **1461:**177–200.